Protein Science (2000), *9*:536–543. Cambridge University Press. Printed in the USA.

Cytochrome *c* folds through a smooth funnel

MARKANDESWAR PANDA, MARIA G. BENAVIDES-GARCIA,
MICHAEL M. PIERCE, AND BARRY T. NALL

Center for Biomolecular Structure, Department of Biochemistry,
University of Texas Health Science Center, 7703 Floyd Curl Drive,
San Antonio, Texas 78229-3900

(RECEIVED July 27, 1999; FINAL REVISION December 8, 1999; ACCEPTED December 20, 1999)

Abstract

A dominant feature of folding of cytochrome *c* is the presence of nonnative His-heme kinetic traps, which either pre-exist in the unfolded protein or are formed soon after initiation of folding. The kinetically trapped species can constitute the majority of folding species, and their breakdown limits the rate of folding to the native state. A temperature jump (T-jump) relaxation technique has been used to compare the unfolding/folding kinetics of yeast iso-2 cytochrome *c* and a genetically engineered double mutant that lacks His-heme kinetic traps, H33N,H39K iso-2. The results show that the thermodynamic properties of the transition states are very similar. A single relaxation time τ_{obs} is observed for both proteins by absorbance changes at 287 nm, a measure of solvent exclusion from aromatic residues. At temperatures near T_m, the midpoint of the thermal unfolding transitions, τ_{obs} is four to eight times faster for H33N,H39K iso-2 ($\tau_{obs} \sim$ 4–10 ms) than for iso-2 ($\tau_{obs} \sim$ 20–30 ms). T-jumps show that there are no kinetically unresolved ($\tau <$ 1–3 μs T-jump dead time) "burst" phases for either protein. Using a two-state model, the folding (k_f) and unfolding (k_u) rate constants and the thermodynamic activation parameters $\Delta G_f^{\ddagger}$, $\Delta G_u^{\ddagger}$, $\Delta H_f^{\ddagger}$, $\Delta H_u^{\ddagger}$, $\Delta S_f^{\ddagger}$, $\Delta S_u^{\ddagger}$ are evaluated by fitting the data to a function describing the temperature dependence of the apparent rate constant k_{obs} ($= \tau_{obs}^{-1}$) $= k_f + k_u$. The results show that there is a small activation enthalpy for folding, suggesting that the barrier to folding is largely entropic. In the "new view," a purely entropic kinetic barrier to folding is consistent with a smooth funnel folding landscape.

Keywords: cytochrome *c*; fast folding; folding landscape; heme ligands; His; iso-2; kinetic traps; nonnative; temperature jump

Recently, there have been a number of publications on the "fast folding" of small globular proteins in the submillisecond time range (Schindler et al., 1995; Hagen et al., 1996, 1997; Chan et al., 1997; Eaton et al., 1997; Takahashi et al., 1997; Yeh et al., 1997; Shastry et al., 1998; Yeh & Rousseau, 1998). Some of these studies have also involved measurements of thermodynamic activation parameters as a means of characterizing folding transition states (Schindler & Schmid, 1996; Yeh et al., 1997). The techniques involved include ultrarapid mixing in which folding is monitored by fluorescence (Chan et al., 1997), or resonance Raman spectroscopy (Takahashi et al., 1997; Yeh et al., 1997; Yeh & Rousseau, 1998). The ultra rapid mixing technique has a dead time of about 80 μs (Eaton et al., 1997). An improved technique (Shastry et al., 1998) called Continuous-Flow Capillary Mixing has a dead time around 40 μs. Other approaches for rapidly initiating folding include laser photodissociation of a cytochrome *c* CO-heme complex and photo-induced electron injection (Jones et al., 1993; Pascher et al., 1996; Hagen et al., 1997; Chen et al., 1998; Goldbeck et al., 1999). The laser-initiated methods are capable of bringing about the conditions needed for folding on a submicrosecond timescale. For example, laser T-jumps with dead times of about 10 ns can measure the kinetics of local cooperative reactions such as helix-coil transitions with $\tau \sim$ 50–160 ns (Williams et al., 1996; Gilmanshin et al., 1997). Nevertheless, most folding reactions occur on a microsecond or longer timescale, probably reflecting the speed limit for forming tertiary contacts in folding (Eaton et al., 1997; Hagen et al., 1997). Capacitive-discharge temperature-jump relaxation is a highly sensitive technique with dead times sufficiently short (1–3 μs) to measure adhesion steps in protein folding in which the tertiary interactions are formed by polypeptide loop closure (Hagen et al., 1996, 1997). T-jumps have the advantage of allowing the study of protein folding in the absence of chemical denaturants that destabilize folding intermediates. Previously, the temperature jump relaxation technique has been used to study folding of cytochrome *c* from horse (Tsong, 1976) and from the yeast *Saccharomyces cerevisiae* (Nall & Landers, 1981; Nall, 1983).

In native cytochrome *c*, His18 and Met80 are the axial ligands of the heme prosthetic group. In unfolded iso-2 near neutral pH, His18 remains coordinated to the heme, whereas Met80 is displaced by a nonnative ligand, His33 or His39. Thus, reformation of

Reprint requests to: Barry T. Nall, Department of Biochemistry AH 5.206, University of Texas Health Science Center-7760, 7703 Floyd Curl Drive, San Antonio, Texas 78229-3900; e-mail: nall@uthscsa.edu.

the native protein requires a ligand exchange reaction in which a nonnative heme ligand, His33 or His39, is replaced by Met80, the native heme ligand. Stopped-flow kinetic studies have compared folding of iso-2 to folding of the double mutant, H33N,H39K iso-2, which folds to the native state without having to displace a nonnative His-heme ligand. The results show that nonnative His-heme ligation acts as a kinetic trap to cytochrome *c* folding (Pierce & Nall, 1997).

Here, we report a temperature-jump kinetic study of the folding/unfolding of yeast iso-2 cytochrome *c* and an iso-2 double mutant lacking the nonnative His heme ligands, H33N,H39K iso-2. One objective is to compare the thermodynamic activation parameters for folding/unfolding involving His-heme kinetic traps (iso-2) to folding/unfolding in the absence of kinetic traps (H33N,H39K iso-2). A second objective is to detect, if present, any additional very fast (submillisecond) events in folding/unfolding on a timescale capable of resolving the kinetics of diffusion-limited adhesion steps in folding (Karplus & Weaver, 1994; Hagen et al., 1996). The physical property used to monitor folding, 287 nm absorbance, measures changes in the polarity of the environment of aromatic groups (e.g., Tyr, Trp, heme, and Phe) on folding/unfolding. Thus, signal changes reflect the formation/disruption of the aromatic hydrophobic core on folding/unfolding.

Results

Equilibrium unfolding

Figure 1 shows the thermal unfolding curves of iso-2 and H33N,H39K iso-2 cytochrome *c* monitored by absorbance at 287 nm. The melting temperature (T_m) for the wild-type and the double mutant is the same, 54 ± 0.2 °C. Thermal unfolding curves monitored by heme absorbance at 394 and 418 nm (data not shown) give similar equilibrium unfolding transitions with the same transition midpoints as the ones shown in Figure 1. The enthalpies ΔH_U generated from the thermal unfolding curves are the same for the two proteins within errors: $\Delta H_U = 71 \pm 2$ kcal mol^{-1} for iso-2 and $\Delta H_U = 68 \pm 2$ kcal mol^{-1} for H33N,H39K iso-2 cytochrome *c*. The data analysis was carried out by least-squares fitting of the absorbance vs. temperature data to a two-state model to obtain the T_m and the ΔH_U (see Materials and methods).

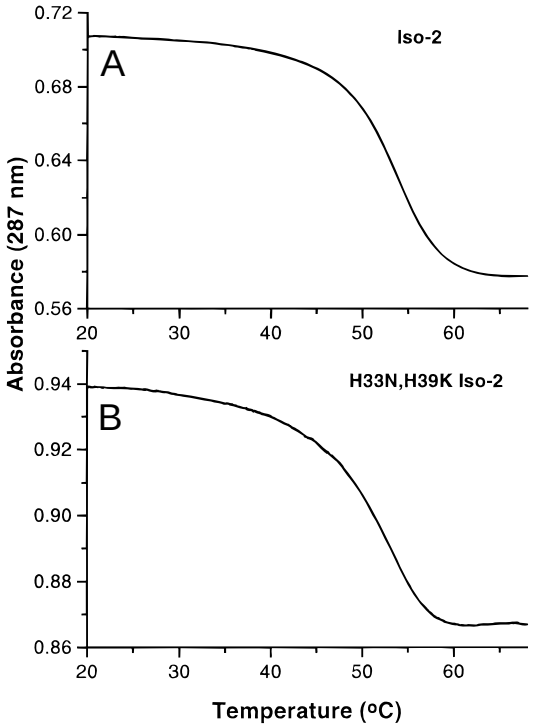

Fig. 1. Equilibrium thermal unfolding curves for (**A**) iso-2 and (**B**) H33N,H39K iso-2 measured at 287 nm. The data were collected on an AVIV 14DS spectrophotometer (AVIV, Lakewood, New Jersey) at a heating rate of 1 °C/min. Essentially identical transitions are observed when samples are incubated for 5 min at each temperature prior to measuring the absorbance. Solution conditions were 30 μM cytochrome *c*, in 0.1 M sodium phosphate, pH 6.0.

Temperature-jump kinetics

Figure 2 presents kinetic transients monitored at 287 nm, after a 5 °C temperature jump. The top panel illustrates the relaxation kinetics of iso-2, which is described by a single exponential function with an apparent rate constant k_{obs} ($= \tau_{obs}^{-1}$) = 32 s^{-1} at a final temperature of 54 °C (T_m). The bottom panel illustrates the relaxation kinetics measured at 287 nm for the H33N,H39K iso-2 protein, which is described by a single exponential function, with an apparent rate constant $k_{obs} = 250$ s^{-1}. All kinetic changes monitored at 287 nm could be described by a single exponential function for both iso-2 and the double mutant. In general, for temperature jumps ending at final temperatures near the melting temperature (T_m = 54 °C) the kinetic phase observed in H33N,H39K iso-2 cytochrome *c* is four to eight times faster than the corresponding kinetic phase observed for iso-2 cytochrome *c*.

Figure 3 plots the apparent rate constant k_{obs} ($= 1/\tau_{obs} = k_u + k_f$) as a function of the final temperature for iso-2 (Fig. 3A) and H33N,H39K iso-2 (Fig. 3B) cytochrome *c*. This figure contains data points obtained from 5 °C temperature jumps at final temperatures that range from 5 °C below to 5 °C above the melting temperature (T_m) of these proteins. Other data points shown in this figure at final temperatures below 310 K (37 °C) were collected using stopped-flow mixing. The stopped-flow experiments are performed under conditions where folding is much more favorable than unfolding, so that $k_{obs} = k_f + k_u \sim k_f$. The stopped-flow data were obtained using two different ways to initiate folding: (1) guanidine hydrochloride dilutions and (2) pH jumps. Both methods give the same values of k_{obs} at the same final temperature, indicating that the small amount of Gdn·HCl (0.27 M Gdn·HCl) present in the final conditions of the Gdn·HCl-dilution experiments does not affect the rate significantly. The temperature dependence of k_{obs} follows a backward L-shaped pattern centered about the T_m. Below T_m the rate constant is almost independent of the final temperature, but at temperatures above T_m the rate constant depends strongly on the final temperature.

Figure 4 shows Eyring plots ($\Delta G^{\ddagger}/T$ vs. $1/T$) for unfolding (Fig. 4A) and for folding (Fig. 4B). The $\Delta G_u^{\ddagger}/T$ and $\Delta G_f^{\ddagger}/T$ functions represent the unfolding and folding components of the apparent rate constant k_{obs} (see Equations 3–6, Materials and methods). The functions $\Delta G_u^{\ddagger}/T$ and $\Delta G_f^{\ddagger}/T$ were calculated from the thermodynamic parameters (Table 1) obtained by fitting the data as described in Materials and methods. The function $\Delta G_u^{\ddagger}/T$ depends strongly on the final temperature because of the large activation enthalpy for unfolding (Fig. 4A). In contrast, $\Delta G_f^{\ddagger}/T$ is

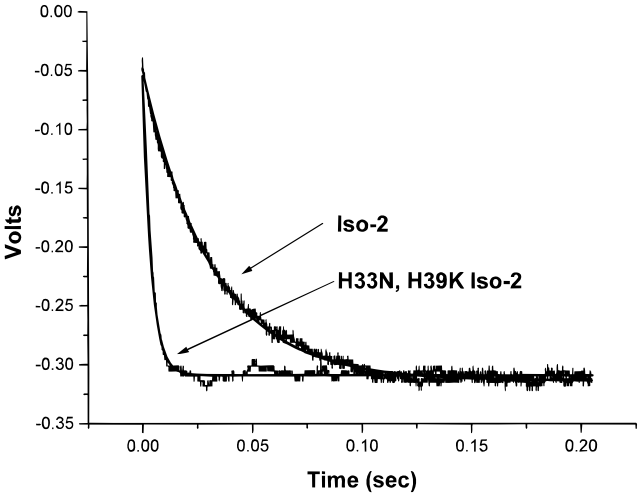

Fig. 2. Relaxation kinetic transients for iso-2 (upper trace) and H33N,H39K iso-2 (lower trace) cytochrome *c* after a 5 °C temperature jump (49 to 54 °C) monitored by absorbance changes at 287 nm. Solution conditions were 30 μM cytochrome *c*, in 0.1 M sodium phosphate, pH 6.0.

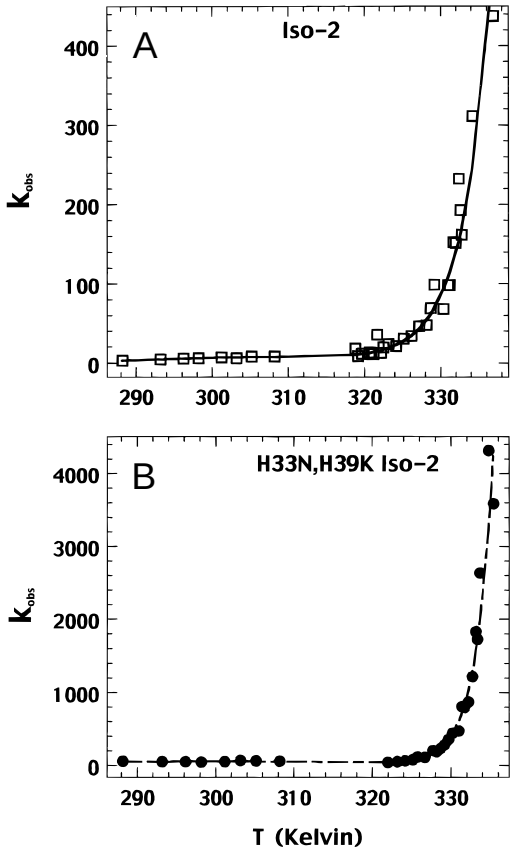

Fig. 3. The temperature dependence of the apparent rate constant k_{obs} ($= \tau_{obs}^{-1}$) for iso-2 (**A**; open squares) and H33N,H39K iso-2 (**B**; filled circles) cytochrome *c* measured with temperature jumps or stopped flow mixing, and monitored by absorbance changes at 287 nm. The solid line in **A** and the dashed line in **B** are fits of the data for iso-2 and H33N,H39K iso-2, respectively, to Equation 6A–C (Materials and methods) with the parameters given in Table 1. In the folding baseline region (below 310 K), the data were obtained by stopped-flow mixing. Above 310 K the data were obtained by 5 K temperature jumps. The experimental conditions for temperature jumps were 30 μM cytochrome *c*, 0.1 M sodium phosphate, pH 6.0. Stopped flow refolding was initiated by pH jumps, or by Gdn·HCl dilution. The Gdn·HCl dilution experiments were carried out by mixing protein solutions in 4.0 M Gdn·HCl in 0.1 M sodium phosphate buffer, pH 6 with 0.1 M sodium phosphate, pH 6.0 using a Biologic SFM-3 stopped-flow instrument so that the final reaction conditions were 0.27 M Gdn·HCl, 0.1 M sodium phosphate, pH 6. For pH jumps the final conditions were 0.1 M sodium phosphate, pH 6. The final protein concentrations were 60 to 75 μM of iso-2 or 70 to 100 μM of H33N,H39K iso-2.

almost independent of the final temperature, i.e., $\Delta H_f^{\ddagger} \sim 0$ (Fig. 4B).

Table 1 lists the thermodynamic parameters obtained from analysis of the equilibrium thermal unfolding curves and the activation parameters calculated from the kinetic data. Iso-2 and H33N,H39K iso-2 have the same melting temperatures (T_m), and the equilibrium unfolding enthalpies and entropies are the same within errors. The equilibrium and activation parameters are given for the reference temperature of $T = T_m$ (54 °C). The equilibrium enthalpy and entropy changes are known to be temperature dependent since calorimetry measurements show that there is a substantial $\Delta C_P = 1.58$ kcal mol^{-1} K^{-1} (McGee et al., 1996). For both proteins the activation parameters for unfolding and folding show that the enthalpic barriers to unfolding are much greater than for folding. The change in the activation free energies, $\Delta G^{\ddagger}$ at $T_m = 54$ °C, were calculated from the activation entropy and enthalpy values generated from the fit of the data in Figure 3 (Materials and methods). The differences between the activation parameters for unfolding and folding are given in square brackets in Table 1 and, assuming a two-state model, can be compared to the equilibrium thermodynamic parameters. According to the analysis using Eyring transition state theory both proteins have positive activation entropies of unfolding and negative activation entropies of folding.

Discussion

Equilibrium unfolding

The thermal unfolding transitions of iso-2 and H33N,H39K iso-2 cytochrome *c* have the same melting temperatures and almost identical enthalpies ΔH_U (Fig. 1). This suggests that substitution of the two histidines (H33N and H39K) does not alter significantly the thermal stability of cytochrome *c*. These thermodynamic parameters are in excellent agreement with thermodynamic values reported in the past for cytochrome *c* (McGee et al., 1996). In a previous study (Pierce & Nall, 1997), Gdn·HCl-induced unfolding transitions showed that H33N,H39K iso-2 was similar in stability to iso-2 in the transition region, but because of a larger *m*-value ($m = d\Delta G_U/d$[Gdn·HCl]) was more stable in the absence of denaturant. Pierce and Nall (1997) pointed out that the removal of the nonnative His-heme ligands is expected to destabilize the unfolded protein by an amount equal to the free energy of the His-heme dissociation reaction and, consequently, increases the unfolding free energy.

Temperature-jump kinetics

The absorbance changes at 287 nm for iso-2 and H33N,H39K iso-2 are well described by a single exponential kinetic phase for all final temperatures. This phase is approximately four to eight

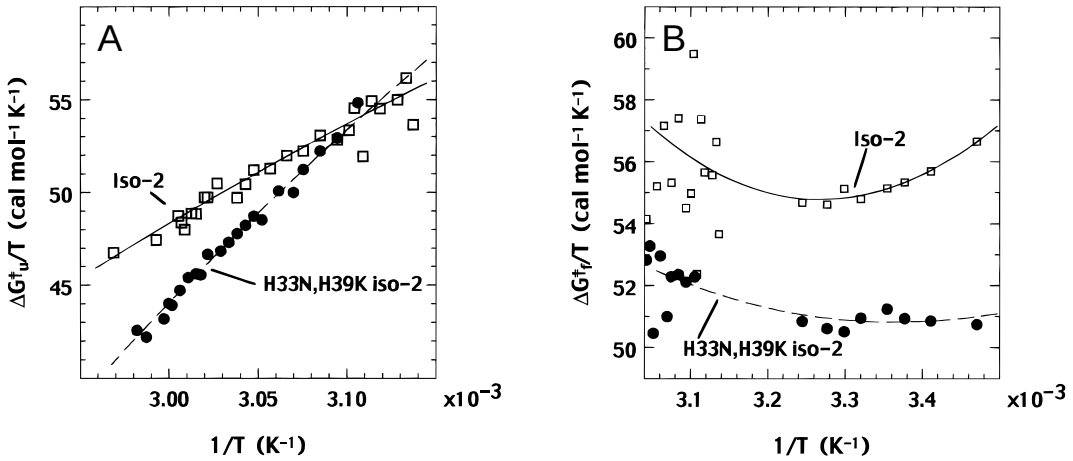

Fig. 4. Eyring plots illustrating (**A**) the strong temperature dependence of unfolding and (**B**) the comparatively weak temperature dependence of folding for iso-2 (solid lines; open squares) and H33N,H39K iso-2 (dashed lines; filled circles). The activation enthalpies are the "slopes" of these plots, while the activation entropies are the Y intercepts at $1/T = 0$. Activation heat capacity changes are obtained from the curvature of the plots. The Eyring plots (solid lines; dashed lines) are calculated using the activation enthalpies, entropies, and heat capacity changes (Table 1; Fig. 3) from the fits of the combined temperature jump and stopped flow data sets to Equation 6A–C (Materials and methods). The data points (open squares for iso-2; filled circles for H33N,H39K iso-2) are obtained by calculating values of k_f or k_u using the activation parameters (Table 1) and subtracting the calculated values from the measured values of k_{obs} ($= k_f + k_u$) to give "measured" values of k_f and k_u. Measured values of $\Delta G^{\ddagger}/T$ are calculated from "measured" k_f or k_u using Equation 3 (Materials and methods).

times faster for H33N,H39K iso-2 ($\tau_{obs} \sim 4$–10 ms) than for iso-2 ($\tau_{obs} \sim 20$–30 ms) at final temperatures near T_m, the melting temperature (Fig. 2). In the two-state approximation for $T = T_m$, $K_u = k_f/k_u = 1$ so $k_f = k_u$, and $k_{obs} = k_f + k_u = 2k_f = 2k_u$. Thus, near T_m, k_f and k_u are both larger (faster) in the absence (H33N,H39K iso-2) than in the presence (iso-2) of nonnative His-heme ligands. So His-heme misligation slows both folding and unfolding, e.g., raises the activation free energies for both reactions. His-heme misligation is known to have slowing effects on folding and unfolding rates measured by Gdn·HCl mixing experiments, where the role of His33 and His39 as kinetic traps has been established by stopped-flow mixing experiments that showed that removal of all nonnative His-heme ligands increased the rate of fast phase folding (Pierce & Nall, 1997) and unfolding (M.M. Pierce & B.T. Nall, unpubl. data) about tenfold.

The observation that the folding and unfolding rates are slowed by nonnative His-heme misligation is consistent with the resonance Raman studies of horse cytochrome *c*, which show that a ligand exchange phase is a common feature of folding (Yeh et al., 1997; Yeh & Rousseau, 1998) and unfolding (Yeh & Rousseau, 1999). Control of both folding and unfolding rates by the ligand exchange phase may explain why a two-state mechanism provides a fair description of the iso-2 folding/unfolding kinetics despite presence of the misligation kinetic block. However, caution is necessary in comparing horse cytochrome *c* and iso-2 because of the greater thermodynamic stability of horse cytochrome *c* and mechanistic differences in coupling of His-heme misligation to folding (M.M. Pierce & B.T. Nall, unpubl. data).

Reliable activation parameters have been obtained by resonance Raman for transitions between distinct heme ligand states in folding of horse cytochrome *c* (Yeh et al., 1997). A comparison of horse and iso-2 folding near 20 °C shows that the changes in the activation enthalpy and entropy between the unfolded protein and the folding transition state for iso-2 are almost identical to the ligand exchange step (TS1) in folding of horse cytochrome *c* where the misligated His is displaced by a water molecule: $\Delta H_f^{\ddagger}(20\,^{\circ}\mathrm{C}) = 13$ kcal mol^{-1} for iso-2; $\Delta H_{TS1}^{\ddagger} = 12$ kcal mol^{-1} for horse cytochrome *c*; $\Delta S_f^{\ddagger}(20\,^{\circ}\mathrm{C}) = -11$ cal mol^{-1} K^{-1} for iso-2; $\Delta S_{TS1}^{\ddagger} = -14$ cal mol^{-1} K^{-1} for horse cytochrome *c*. The agreement may be fortuitous, or it may be a further indication of control of the iso-2 folding rate by His-heme ligand exchange.

Assuming that His-heme displacement is rate-limiting, the activation enthalpy for iso-2 folding can also be compared to activation energies for His-heme ligand off rates measured for unfolded horse cytochrome *c*. Distinct kinetic processes in the millisecond time range were detected for the His26–heme off rate and the His33–heme off rate with activation energies of 12 and 17 kcal mol^{-1}, respectively (Colon et al., 1997).

Burst phases and two-state models of folding

Submillisecond mixing measurements of horse cytochrome *c* folding (Shastry & Roder, 1998; Shastry et al., 1998) have resolved a "burst" phase in folding into a submillisecond kinetic phase believed to represent chain collapse. Also, a microsecond T-jump relaxation process has been reported for fully unfolded horse cytochrome *c* (Tsong, 1975, 1977). Interestingly, the kinetic process detected in the fully unfolded protein is in the same time range ($\tau \sim 50$ μs) as the "collapse" phase detected by submillisecond mixing measurements of horse cytochrome *c* folding, suggesting that the "burst" phase may be a reaction within the ensemble of unfolded species that couples to folding under strong refolding conditions. This view is supported by the fact that the amplitude of the submillisecond phase decreases to near zero as the final denaturant concentration approaches the unfolding transition zone (Shastry & Roder, 1998).

Stopped flow measurements of refolding of iso-2 and iso-2 variants also exhibit substantial burst phases (Nall, 1983; Pierce &

Table 1. *Equilibrium and kinetic thermodynamic parameters for iso-2 and H33N,H39K iso-2*[a]

Thermodynamic parameter	Protein	
	Iso-2	H33N,H39K iso-2
Equilibrium		
T_m (°C)	54.0 ± 0.2	54.0 ± 0.2
ΔH_U° (kcal mol^{-1})	71 ± 2	68 ± 2
	[75 ± 10][b]	[103 ± 6][b]
ΔS_U° (cal mol^{-1} K^{-1})	217 ± 2	208 ± 2
	[233 ± 31][b]	[319 ± 17][b]
ΔC_P (kcal mol^{-1} K^{-1})	1.58	1.58
ΔG_U° (kcal mol^{-1})	0	0
	[−1.7 ± 14][b]	[−1.0 ± 8][b]
Kinetic		
$\Delta H_f^\ddagger$ (kcal mol^{-1})	−21 ± 9	−11 ± 4
$\Delta S_f^\ddagger$ (cal mol^{-1} K^{-1})	−122 ± 29	−86 ± 13
$\Delta C_{P,f}^\ddagger$ (kcal mol^{-1} K^{-1})	−1.0 ± 0.3	−0.4 ± 0.2
$\Delta G_f^\ddagger$ (kcal mol^{-1})	18.6 ± 13	17.2 ± 6
$\Delta H_u^\ddagger$ (kcal mol^{-1})	53 ± 4	92 ± 4
$\Delta S_u^\ddagger$ (cal mol^{-1} K^{-1})	111 ± 11	233 ± 11
$\Delta C_{P,u}^\ddagger$ (kcal mol^{-1} K^{-1})	0.6 ± 0.3	1.2 ± 0.2
$\Delta G_u^\ddagger$ (kcal mol^{-1})	16.8 ± 6	16.1 ± 6

[a]Thermodynamic parameters at $T_m = 54$ °C, the midpoint of the thermal unfolding transition. The equilibrium thermodynamic parameters are obtained by fitting the data (Fig. 1A,B) as described in Materials and methods to obtain the enthalpy and entropy values at T_m (327.16 K). Equilibrium free energies are assumed to be zero at $T_m = 54$ °C (327.16 K). The kinetic (activation) thermodynamic parameters were obtained by fitting the data of Figures 3A and 3B to Equation 6 (Materials and methods). The activation parameters for heat capacity changes, $\Delta C_{P,f}^\ddagger$ (folding) and $\Delta C_{P,u}^\ddagger$ (unfolding), are assumed to be independent of temperature. The optimized fitting function is shown by the solid line in Figures 3A and 3B. The errors in the enthalpies and entropies are obtained from the statistical errors of the fits. Errors in the equilibrium and activation free energies are propagated from the errors in the enthalpy and entropy. In fitting the data, the difference in the activation heat capacity changes ($\Delta C_{P,u}^\ddagger - \Delta C_{P,f}^\ddagger$) was constrained to the known equilibrium value of $\Delta C_P = 1.58$ kcal mol^{-1} K^{-1} determined by scanning calorimetry of normal and mutant variants of iso-1 and iso-2 (McGee et al., 1996; Liggins et al., 1999).

[b]The equilibrium thermodynamic parameters shown in square brackets are calculated from differences between the corresponding thermodynamic activation parameters, e.g., $\Delta G_U = \Delta G_u^\ddagger - \Delta G_f^\ddagger$.

Nall, 1997; McGee & Nall, 1998), suggesting that an analogous submillisecond phase should be observed by temperature jumps of iso-2. There are no faster phases observed by 287 nm absorbance. Moreover, if such a phase were present with an amplitude above the noise level, it would have been detected in the T-jump experiments. Unlike stopped-flow mixing where the reacting solutions go unobserved during the mixing time, the T-jump absorbance signal is measured before, during, and after the temperature jump, so the amplitude of a kinetic phase faster than the T-jump rise time is detected directly as a signal change with $\tau \sim 3$ μs, the instrument rise time. None are observed. However, the absence of a T-jump detected burst phase may be because of the detection method: 287 nm absorbance for the T-jumps vs. tryptophan fluorescence for the stopped flow experiments. Ultraviolet absorbance measures changes in the polarity of the environment of aromatic residues including heme; i.e., solvent exclusion from the hydrophobic core. Tryptophan fluorescence for cytochrome *c* measures overall Trp-heme (donor-quencher) distance and, in contrast to ultraviolet absorbance, is expected to be sensitive to polymer collapse to condensed solvated species. An additional fast kinetic phase with a time constant, $\tau \sim 1$ ms ($k_{obs} \sim 1{,}000$ s^{-1}) has been detected by T-jump measurements of iso-2 folding/unfolding monitored by absorbance at 418 nm. The phase is detected by heme absorbance changes, but not by fluorescence emission ($\alpha < 0.08$ at 350 nm) or ultraviolet absorbance ($\alpha < 0.04$ at 287 nm) (Nall & Landers, 1981; Nall, 1983) suggesting that the process involves changes in heme environment or ligation state within the ensemble of unfolded species. It is surprising that fluorescence-detected T-jumps do not detect the faster phase, but since initial conditions differ for the stopped-flow and the temperature-jump experiments, the amplitudes can also differ. Thus, the kinetic phase detected by stopped-flow might have an undetectably small amplitude when measured by temperature jumps.

The present T-jump measurements of changes in ultraviolet absorbance (287 nm), in accord with our previous results (Nall, 1983), detect a single kinetic phase. We believe that the phase detected by T-jumps is the rate-limiting structural phase in which solvent is excluded from the hydrophobic core, and that a two-state model is a fair representation of the process within or near the unfolding transition zone. However, folding or unfolding measured far removed from the transition region could deviate significantly from a two-state mechanism. Some indications of deviations are the burst phase detected by stopped-flow mixing under strongly native conditions, and discrepancies between the equilibrium thermodynamic parameters and the differences in the thermodynamic activation parameters (Table 1).

Activation parameters

The activation parameters for unfolding and folding (Table 1) and Eyring plots of activation free energies (Fig. 4A,B) show that the temperature dependence of unfolding is much larger than folding for both proteins. Although the activation $\Delta C_{P,f}^\ddagger$ leads to curvature of the Eyring plots, $\Delta G_f^\ddagger/T$ is almost independent of temperature over the refolding temperature range, especially in the case of H33N,H39K iso-2 (Fig. 4B; Table 1). The temperature dependence of unfolding ($\Delta G_u^\ddagger/T$) is much stronger than refolding in both a relative and absolute sense (Fig. 4A; Table 1). This suggests that most of the change in (equilibrium) enthalpy occurs between the transition state and the folded state, implying that the enthalpy of the transition state is similar to that of the unfolded protein.

A similar comparison of activation entropies is complicated by the frequency factor in Eyring theory that shows up primarily in the activation entropy. It is unlikely that the factor ($\nu = k_B T/h$) used in the usual Eyring analysis is appropriate for protein folding. The frequency factor, which gives a measure of the reaction rate in the absence of a barrier (enthalpic or entropic), is meant to apply to gas phase reactions of small molecules. A recent review (Jacob & Schmid, 1999) of rate theory for folding reactions concludes that the calculated absolute rates are much too high so the (absolute) values of $\Delta G^\ddagger$ and $\Delta S^\ddagger$ obtained from rate constants are not reliable. However, Eyring theory is useful in quantifying changes in these same quantities that arise from mutation or differences in solution conditions. The alternative Kramers' theory was developed for reactions in solution and may be better suited to the analysis of many aspects of folding. For simple folding processes, Kramers' theory predicts that rates will be inversely proportional to solvent viscosity, as observed for folding of CspB (Jacob et al.,

1999). Regardless of the uncertainties in absolute values, the very low activation enthalpies for folding in the present case (Fig. 4B) lead to the conclusion that the barrier to folding is largely entropic.

The activation heat capacity changes ($\Delta C_P^{\ddagger}$) are the least accurately measured of all the parameters. To obtain statistically significant values from the fits of the data, it was necessary to constrain the difference between the activation heat capacity changes to the independently determined equilibrium value: $\Delta C_P \equiv \Delta C_{P,u}^{\ddagger} - \Delta C_{P,f}^{\ddagger}$. There is a significant $\Delta C_P^{\ddagger}$ for both folding and unfolding. Removal of His-heme misligation shifts the point at which the largest part of the folding ΔC_P change occurs from between the unfolded state and the transition state to between the transition state and the native state: $|\Delta C_{P,f}^{\ddagger}|/\Delta C_P \sim 0.6$ for iso-2; $|\Delta C_{P,f}^{\ddagger}|/\Delta C_P \sim 0.3$ for H33N,H39K iso-2. Although the errors in $\Delta C_{P,f}^{\ddagger}$ are large, the implication is that elimination of His-heme misligation leads to a more solvent-exposed transition state with a thermodynamic character closer to that of the unfolded protein.

Conclusions

The results show that the enthalpic barriers of the transition states for folding of iso-2 and H33N,H39K iso-2 are similar to one another and to the unfolded state. This is despite the fact that disruption of incorrect His-heme kinetic traps are rate-limiting for iso-2 folding, while folding of H33N,H39K iso-2 takes place in the absence of His-heme kinetic traps. For both proteins the barrier to folding is largely entropic, which in the "new view" implies that the energy landscape for folding is a smooth funnel.

Materials and methods

The construction, purification, and characterization of iso-2 and the mutant H33N,H39K iso-2 cytochrome *c* have been previously described (Pierce & Nall, 1997).

Equilibrium unfolding

Thermal unfolding curves were obtained using an AVIV model 14DS UV-VIS spectrophotometer (AVIV, Lakewood, New Jersey). The absorbance at 287 nm was measured at a heating rate of 1 °C/min. Protein concentrations were ~30 μM in 0.1 M sodium phosphate, pH 6.0. The protein samples were prepared by dissolving lyophilized cytochrome *c* in a small volume (0.5 mL) of 4 M Gdn·HCl (guanidine hydrochloride) in 0.1 M sodium phosphate, pH 6.0. The samples were warmed in a water bath at 55 °C for 5 min and passed through a G-25 gel filtration column pre-equilibrated with 0.1 M sodium phosphate, pH 6.0 to remove the guanidine hydrochloride.

Analysis of equilibrium thermal transitions

The equilibrium unfolding transitions (Fig. 1A,B) were fit to an equilibrium two-state model using the equation:

$$Y(T) = [(Y_N + m_N T) + (Y_D + m_D T)A]/[1 + A]$$

where A is given by

$$A = \exp[(\Delta H_U/R)((1/T_m) - (1/T))].$$

The function $Y(T)$ describes the temperature dependence of the absorbance measured at 287 nm. Y_N and m_N are the intercept and slope of the baseline for the temperature dependence of the fully native protein, while Y_D and m_D are the corresponding parameters for the unfolded protein baseline. T_m is the temperature midpoint of the thermal unfolding transition and ΔH_U is the unfolding enthalpy at $T = T_m$. T is the temperature in Kelvin and R is the gas constant. The entropy of unfolding at T_m was calculated as $\Delta S_U(T_m) = \Delta H_U/T_m$. This model assumes that ΔH_U is independent of temperature over the narrow temperature range in which the transition is measured. We have shown that ΔH_U depends on temperature ($\Delta C_P = 1.58$ kcal mol^{-1} K^{-1}) when measurements are made over a wider temperature range (Liggins et al., 1994; McGee et al., 1996).

Temperature-jump kinetics

Relaxation kinetics were measured with a capacitive-discharge (Eigen–DeMayer) temperature-jump instrument (Messanlagen, Germany). The absorbance calibration of the T-jump instrument was carried out using Phenol Red dye in 0.1 M Tris $HClO_4$ buffer (pH 7.4). The absorbance of the dye solutions at various concentrations was measured at 558 nm in the T-jump instrument and in the AVIV UV-VIS spectrophotometer. The absorbance in the T-jump was in fair agreement with that expected for the shorter (0.7 cm) path length of the T-jump sample cell. A temperature calibration curve was obtained by measuring the change in absorbance at 558 nm of the dye solution vs. temperature in the AVIV model 14DS UV-VIS spectrophotometer. The magnitude of the "rise-time" signal change for the dye solution in the T-jump cell was measured as a function of the voltage used to charge the 0.05 μF capacitor. Using the T-jump absorbance calibration, the signal changes were converted to absorbance changes in the AVIV spectrophotometer, and the temperature calibration curve used to convert the absorbance changes to changes in temperature. It was determined that a 28 kV discharge from the 0.05 μF capacitor generates a 5 °C temperature jump under experimental conditions. The rise time (dead time) of the instrument was determined to be 3 μs with the phenol red dye solution.

The protein solutions used were 30 μM cytochrome *c*, 0.1 M sodium phosphate buffer, pH 6.0. The data were analyzed using the Origin software program (MicroCal, version 2.9). The kinetic transients were fit to the function: $A(t) = A_1 \exp(-k_{obs}t) + C$, where $A(t)$ is the experimentally observed absorbance at time t, A_1 is the amplitude of the kinetic phase, k_{obs} is the observed rate constant, and C is the offset voltage. In the nonlinear least-squares fit, all the parameters (A_1, k_{obs}, and C) were allowed to float until a minimum was reached.

Stopped-flow kinetics

The stopped-flow experiments were carried out using a three syringe Biologic SFM-3 stopped-flow (Molecular Kinetics, Inc., Pullman, Washington). The Gdn·HCl-jump experiments were carried out by mixing protein unfolded in 4 M Gdn·HCl, 0.1 M sodium phosphate buffer, pH 6.0 with mixing buffer of 0.1 M sodium phosphate, pH 6.0, so that the final reaction conditions were 60–75 μM iso-2 or 70–100 μM H33N,H39K iso-2, 0.27 M Gdn·HCl, and 0.1 M sodium phosphate, pH 6.0. A 10 mm light path zigzag cuvette (TC-100-15, Biologic) was used for the experiments in which folding was monitored by absorbance at 287 nm. For the pH-jump experiments, the initial conditions were 650 to

800 μM cytochrome *c*, 10 mM HCl, pH 2.3. The mixing buffer was 0.1 M sodium phosphate buffer, pH 6.2. Following the 1:9 dilution with mixing buffer, the final conditions were 65 to 80 μM cytochrome *c*, 0.1 M sodium phosphate, pH 6.1.

Analysis of kinetics

For the two-state folding reaction shown in Equation 1:

$$N \underset{k_u}{\overset{k_f}{\leftrightarrows}} U \tag{1}$$

the apparent rate constant k_{obs} ($= \tau_{obs}^{-1}$) is equal to the sum of the microscopic rate constants of unfolding k_u and folding k_f (Equation 2).

$$k_{obs} = k_u + k_f. \tag{2}$$

Transition state theory relates individual rate constants to the change in the Gibbs free energy between the initial state and the transition state by Equation 3:

$$k = (k_B T/h)\exp(-\Delta G^{\ddagger}/RT) \tag{3}$$

where k is either k_u, the microscopic rate constant for unfolding, or k_f, the microscopic rate constant for folding, k_B is the Boltzmann constant, h is Planck's constant, T is the (absolute) temperature, and R is the gas constant. The activation free energy can be decomposed into its enthalpic and entropic components (Equation 4):

$$\Delta G^{\ddagger} = \Delta H^{\ddagger} - T\Delta S^{\ddagger}. \tag{4}$$

Combining Equations 3 and 4, we get the following expression (Equation 5):

$$k = (k_B T/h)\exp\{(\Delta S^{\ddagger}/R) - (\Delta H^{\ddagger}/RT)\}. \tag{5}$$

Combining Equations 2 and 5, we obtain k_{obs} in terms of the activation enthalpies and entropies of unfolding and folding (Equation 6):

$$k_{obs} = (k_B T/h)[\exp\{(\Delta S_u^{\ddagger}/R) - (\Delta H_u^{\ddagger}/RT)\} + \exp\{(\Delta S_f^{\ddagger}/R) - (\Delta H_f^{\ddagger}/RT)\}]. \tag{6A}$$

To account for the temperature dependence, the activation enthalpies and entropies were expressed as (Schellman, 1987)

$$\Delta H^{\ddagger}(T) = \Delta H_m^{\ddagger} + \Delta C_P^{\ddagger}(T - T_m) \tag{6B}$$

$$\Delta S^{\ddagger}(T) = \Delta S_m^{\ddagger} + \Delta C_P^{\ddagger} \ln(T/T_m) \tag{6C}$$

where the subscript m refers to the reference temperature $T = T_m$ ($= 54\,^{\circ}\mathrm{C}$).

Equation 6A–C was entered into a nonlinear least-squares fitting program: Origin 5.0 (MicoCal, Inc., Northampton, Massachusetts); or Horizon (David Guenther, V. 1.5). The activation parameters for unfolding and folding of both proteins were determined by fitting the measured values of $k_{obs}(T)$ to Equation 6.

Acknowledgments

The authors thank Dr. Susan Weintraub for help with the electrospray ion mass spectrometry and Sofia Ghidarpour for help in construction of mutant iso-2 containing yeast strains. William A. McGee and C.S. Raman provided advice on kinetic methods and instrumentation. The work was supported by grants from the National Institute of General Medical Sciences (GM32980), the National Center for Research Resources (RR05043), and the Robert A. Welch Foundation (AQ838).

References

Chan CK, Hu Y, Takahashi S, Rousseau DL, Eaton WA, Hofrichter J. 1997. Submillisecond protein folding kinetics studied by ultrarapid mixing. *Proc Natl Acad Sci USA 94*:1779–1784.

Chen E, Wood MJ, Fink AL, Kliger DS. 1998. Time-resolved circular dichroism studies of protein folding intermediates of cytochrome c. *Biochemistry 37*:5589–5598.

Colon W, Wakem LP, Sherman F, Roder H. 1997. Identification of the predominant non-native histidine ligand in unfolded cytochrome c. *Biochemistry 36*:12535–12541.

Eaton WA, Munoz V, Thompson PA, Chan CK, Hofrichter J. 1997. Submillisecond kinetics of protein folding. *Curr Opin Struct Biol 7*:10–14.

Gilmanshin R, Williams S, Callender RH, Woodruff WH, Dyer RB. 1997. Fast events in protein folding: Relaxation dynamics of secondary and tertiary structure in native apomyoglobin. *Proc Natl Acad Sci USA 94*:3709–3713.

Goldbeck RA, Thomas YG, Chen E, Esquerra RM, Kliger DS. 1999. Multiple pathways on a protein-folding energy landscape: Kinetic evidence. *Proc Natl Acad Sci USA 96*:2782–2787.

Hagen SJ, Hofrichter J, Eaton WA. 1997. Rate of intrachain diffusion of unfolded cytochrome *c*. *J Phys Chem B 101*:2352–2365.

Hagen SJ, Hofrichter J, Szabo A, Eaton WA. 1996. Diffusion-limited contact formation in unfolded cytochrome *c*: Estimating the maximum rate of protein folding. *Proc Natl Acad Sci USA 93*:11615–11617.

Jacob M, Geeves M, Holtermann G, Schmid FX. 1999. Diffusional barrier crossing in a two-state protein folding reaction. *Nat Struct Biol 6*:923–926.

Jacob M, Schmid FX. 1999. Protein folding as a diffusional process. *Biochemistry 38*:13773–13779.

Jones CM, Henry ER, Hu Y, Chan CK, Luck SD, Bhuyan A, Roder H, Hofrichter J, Eaton WA. 1993. Fast events in protein folding initiated by nanosecond laser photolysis. *Proc Natl Acad Sci USA 90*:11860–11864.

Karplus M, Weaver DL. 1994. Protein folding dynamics: The diffusion-collision model and experimental data. *Protein Sci 3*:650–668.

Liggins JR, Lo TP, Brayer GD, Nall BT. 1999. Thermal stability of hydrophobic heme pocket variants of oxidized cytochrome *c*. *Protein Sci 8*:2645–2654.

Liggins JR, Sherman F, Mathews AJ, Nall BT. 1994. Differential scanning calorimetric study of the thermal unfolding transitions of yeast iso-1 and iso-2 cytochromes *c* and three composite isozymes. *Biochemistry 33*:9209–9219.

McGee WA, Nall BT. 1998. Refolding rate of stability-enhanced cytochrome *c* is independent of thermodynamic driving force. *Protein Sci 7*:1071–1082.

McGee WA, Rosell FI, Liggins JR, Rodriguez-Ghidarpour S, Luo Y, Chen J, Brayer GD, Mauk AG, Nall BT. 1996. Thermodynamic cycles as probes of structure in unfolded proteins. *Biochemistry 35*:1995–2007.

Nall BT. 1983. Structural intermediates in folding of yeast iso-2 cytochrome *c*. *Biochemistry 22*:1423–1429.

Nall BT, Landers TA. 1981. Guanidine hydrochloride induced unfolding of yeast iso-2 cytochrome *c*. *Biochemistry 20*:5403–5411.

Pascher T, Chesick JP, Winkler JR, Gray HB. 1996. Protein folding triggered by electron transfer. *Science 271*:1558–1560.

Pierce MM, Nall BT. 1997. Fast folding of cytochrome *c*. *Protein Sci 6*:618–627.

Schellman JA. 1987. The thermodynamic stability of proteins. *Annu Rev Biophys Biophys Chem 16*:115–137.

Schindler T, Herrler M, Marahiel MA, Schmid FX. 1995. Extremely rapid protein folding in the absence of intermediates. *Nat Struct Biol 2*:663–673.

Schindler T, Schmid FX. 1996. Thermodynamic properties of an extremely rapid protein folding reaction. *Biochemistry 35*:16833–16842.

Shastry MC, Luck SD, Roder H. 1998. A continuous-flow capillary mixing method to monitor reactions on the microsecond time scale. *Biophys J 74*:2714–2721.

Shastry MC, Roder H. 1998. Evidence for barrier-limited protein folding kinetics on the microsecond time scale. *Nat Struct Biol 5*:385–392.

Takahashi S, Yeh SR, Das TK, Chan CK, Gottfried DS, Rousseau DL. 1997. Folding of cytochrome *c* initiated by submillisecond mixing. *Nat Struct Biol 4*:44–50.

Tsong TY. 1975. An acid induced conformational transition of denatured cyto-

chrome *c* in urea and guanidine hydrochloride solutions. *Biochemistry 14*:1542–1547.

Tsong TY. 1976. Ferricytochrome *c* chain folding measured by the energy transfer of tryptophan 59 to the heme group. *Biochemistry 15*:5467–5473.

Tsong TY. 1977. Conformational relaxations of urea- and guanidine hydrochloride-unfolded ferricytochrome *c*. *J Biol Chem 252*:8778–8780.

Williams S, Causgrove TP, Gilmanshin R, Fang KS, Callender RH, Woodruff WH, Dyer RB. 1996. Fast events in protein folding: Helix melting and formation in a small peptide. *Biochemistry 35*:691–697.

Yeh SR, Rousseau DL. 1998. Folding intermediates in cytochrome *c*. *Nat Struct Biol 5*:222–228.

Yeh SR, Rousseau DL. 1999. Ligand exchange during unfolding of cytochrome *c*. *J Biol Chem 274*:17853–17859.

Yeh SR, Takahashi S, Fan B, Rousseau DL. 1997. Ligand exchange during cytochrome *c* folding. *Nat Struct Biol 4*:51–56.